

Self-consolidating concrete filled steel tube columns – Design equations for confinement and axial strength

M. Lachemi[†] and K. M. A. Hossain[‡]

Department of Civil Engineering, Ryerson University, 350 Victoria St, Toronto, ON, Canada, M5B 2K3

V. B. Lambros^{‡†}

Lafarge Materials & Construction Inc., Toronto, ON, Canada

(Received August 11, 2004, Accepted December 16, 2005)

Abstract. This paper compares the performance of axially loaded concrete filled steel tube (CFST) columns cast using a conventionally vibrated normal concrete (NC) and a novel self-consolidating concrete (SCC) made with a new viscosity modifying admixture (VMA). A total of sixteen columns with a standard compressive strength of about 50 MPa for both SCC and NC were tested by applying concentric axial load through the concrete core. Columns were fabricated without and with longitudinal and hoop reinforcement (Series I and Series II, respectively) in addition to the tube confinement. The slenderness of the columns expressed as height to diameter ratio (H/D) ranged between 4.8 and 9.5 for Series CI and between 3.1 and 6.5 for Series CII. The strength and ductility of SCC columns were found comparable to those of their NC counterparts as the maximum strength enhancement in NC columns ranged between 1.1% and 7.5% only. No significant difference in strain development was found due to the presence of SCC or NC or due to the presence of longitudinal and hoop reinforcement. Biaxial stress development in the steel tube as per von Mises yield criterion showed similar characteristics for both SCC and NC columns. The confined strength (f'_{cc}) of SCC was found to be lower than that of NC and f'_{cc} also decreased with the increase of slenderness of the columns. Analytical models for the prediction of confined concrete strength and axial strength of CFST columns were developed and their performance was validated through test results. The proposed models were found to predict the axial strength of CFST columns better than existing models and Code based design procedures.

Keywords: self-consolidating concrete; concrete filled tube column; biaxial stress; confinement; axial strength; design equations.

1. Introduction

Self-consolidating concrete (SCC) is a highly flowable high performance concrete (HPC) that can flow into place under its own weight and achieve good consolidation without internal or external vibration and without exhibiting defects due to segregation and bleeding. SCC was developed in

[†] Associate Professor and Canada Research Chair in Sustainable Construction

[‡] Adjunct Professor, Corresponding author, E-mail: ahossain@ryerson.ca

^{‡†} Agilia Specialist

Japan in the late 1980's to be mainly used for highly congested reinforced structures in seismic regions (Ozawa *et al.* 1989). Recently, SCC has gained wide use in many countries for different applications and structural configurations (Khayat *et al.* 1997, 2001, Arima *et al.* 1994, Bouzoubaâ and Lachemi 2001). Recent research carried out at Ryerson University lead to the development of cost-effective SCCs by incorporating either supplementary cementing materials such as fly ash (FA) and slag cement or novel viscosity-modifying agents (VMA) with desirable fresh and hardened properties (Lachemi *et al.* 2003).

Lack of information regarding in-situ properties and structural performance of SCC is one of the main barriers to its acceptance in the construction industry. Limited published studies dealing with the structural performance of SCC demand initiation of new research (Khayat *et al.* 1997, 2001, Arima *et al.* 1994). Current research at Ryerson University is focused on the development of new cost-effective SCCs and their performance in various structural elements both in construction and service stages including both short and long term investigations (Lachemi *et al.* 2003, 2004a, 2004b, Patel *et al.* 2004, Hossain *et al.* 2004).

As part of the ongoing research program, investigations were conducted on the structural performance of concrete-filled steel tube (CFST) columns cast with a newly developed VMA SCC compared to similar columns cast with conventionally vibrated normal concrete (NC) of equal strength. The use of concrete-filled steel tubes (CFSTs) in high rise buildings has become more popular in recent years as they provide several advantages over reinforced concrete or steel columns (Campione *et al.* 2000, Hossain 2003, Gardner and Jacobson 1967, Shakir-Khalil and Mouli 1990, Lahlou and Aïtcin 1997, O'Shea and Bridge 2000, Lahlou *et al.* 1999). CFSTs are an economical alternative to other columns and can become more economical with the use of high performance concrete and thin walled steel tubes. For thicker-walled steel tubes filled with concrete with low to medium strength, increased capacity through concrete confinement can be achieved as indicated in Eurocode 4 (1992). This form of construction combines the compressive strength of concrete with the stiffness and ductility of steel. This blend of properties makes the CFST potentially useful for application in seismic regions.

CFST columns can be classified as Type A where load is applied through both steel and concrete and Type B where load is applied through concrete core only. In North America, design guidance for Type A CFST columns is currently found in the steel design Codes AISC-LRFD 94 (AISC 1994) and CSA S16.1-94 (CSA 1994). The Canadian standard determines the resistance of the column by superposition, whereas the American standard uses a transformed section approach. Regardless, each of these standards is based on the behaviour of steel tubes filled with NC. Their applicability to CFSTs filled with SCC has not been established.

This paper presents a comparative performance study of Type B CFST columns under axial loading illustrating the performance of SCC and NC. The performance is evaluated based on load-displacement response, stress-strain characteristics, degree of confinement, ultimate strength, and failure modes. The effect of various parameters such as slenderness ratios and addition of longitudinal and hoop reinforcements is also presented. Additionally, the experimental program is developed to examine the link between the behaviour of steel tube with that of the confined concrete. The mechanical response of the tube is examined by the evolution of strains under increasing load, while the behaviour of the concrete is quantified by its axial stress-strain curve, and confined strength. Analytical models for the prediction of confined concrete strength and axial strength of CFST columns with different degree of confinement are derived and their performance is validated through experimental results and existing models as well as various Code based design

procedures. The study presented in this paper is a part of a major research project that seeks to evaluate the structural performance of various structural systems using SCC.

2. Background research

Under Type A loading, CFST behaviour can be seen as an enhanced steel tube, while for Type B, it is more properly described as an optimized concrete section (McAteer *et al.* 2004). As the load is applied in Type B column, steel tube-concrete friction causes some axial strain to be transferred from the concrete to the steel tube. Previous research on Type B indicates that the axial steel strain develops as a nonlinear function of the concrete axial strain (Lahlou and Aïtcin 1997, Lahlou *et al.* 1999, Mei *et al.* 2001). Combined with the transverse strain associated with concrete dilation, the steel tube is placed in a state of biaxial stress lowering the von-Mises yield stress in both principal directions. Mei *et al.* (2001) reported that the load sharing by the steel tube in Type B columns decreases as tube D/t ratio increases. For a given concrete, the peak strength and ductility of the column increases in proportion to both tube thickness and uniaxial yield stress (Lahlou and Aïtcin 1997, Lahlou *et al.* 1999, Mei *et al.* 2001). When load sharing is reduced by lubricating the tube interior, the peak capacity of a Type B column can be greater than an identical, non-lubricated column. This has been found true of columns filled with NC (Sun and Sakino 1998), as well as high strength concrete (HSC) (McAteer *et al.* 2004). When compared to an identical Type A column, the peak capacity of a Type B column has been found to be similar (Gardner and Jacobson 1967) or in some cases, slightly greater (Lahlou and Aïtcin 1997, Sun and Sakino 1998).

Given the fundamental difference in the axial resistance mechanism (the steel does not directly participate in resisting the applied load, and thus the axial stiffness of a Type B is less than that of a Type A CFST (Sun and Sakino 1998)), the applicability of current design standards to Type B columns is questionable. If design guidelines are to be drafted for Type B columns specially filled with a novel SCC, a clear understanding of key aspects of performance (peak load capacity, strain at peak, ductility, and failure modes) is required. An understanding of the interactions between steel and concrete is also mandated (McAteer *et al.* 2004).

3. Experimental program

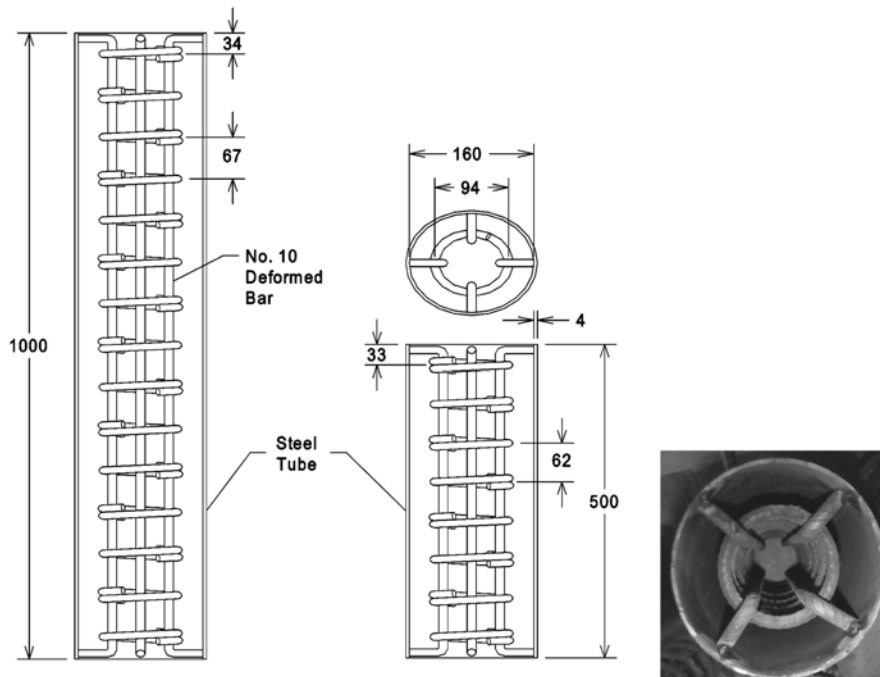
The experimental program consisted of casting CFST columns (with SCC or NC as concrete infill) in two series having different configurations based on the presence or absence of longitudinal and hoop reinforcements. CFST columns in Series CI had concrete infill only while those in Series CII had both longitudinal and hoop reinforcements in addition to concrete infill.

Details of all the columns are presented in Table 1 where the numeric in the column designation represents height to diameter ratio (H/D). Both Series CI and CII columns were made of 4.4 mm thick (t) steel tubes. H/D ratios of Series CI columns were 4.8 and 9.5 while H/D of Series CII columns were 3.1 and 6.3. For each H/D, four columns were cast: two with SCC and two with NC. Series I columns had neither longitudinal nor lateral (hoop) reinforcements. All columns in Series II, were made with 2% longitudinal reinforcement and approximately the same amount of lateral or hoop reinforcement (2.8% and 2.9%). Hoops and longitudinal reinforcements (fabricated from No. 10 deformed bars) were tack welded together and their details are presented in Fig. 1. To prevent

Table 1 Column and material specifications

Column designation	No. of columns	Concrete		Geometry of columns		Reinforcing steel		
		f'_c MPa	E_c GPa	H mm	H/D	Axial %	Hoop %	Total steel %
Series CI: $D = 114$ mm, $t = 4.4$ mm, $f_y: 300$ MPa, $E_s: 200$ GPa								
CI-SCC-4.8	2	54	33.8	500	4.8	-	-	-
CI-NC-4.8	2	52	32.9	500	4.8	-	-	-
CI-SCC-9.5	2	54	33.8	1000	9.5	-	-	-
CI-NC-9.5	2	52	32.9	1000	9.5	-	-	-
Series CII: $D = 168$ mm, $t = 4.4$ mm, $f_y: 300$ MPa, $E_s: 200$ GPa, $f_{yr}: 400$ MPa								
CII-SCC-3.1	2	49	33.9	500	3.1	2.0	2.9	4.9
CII-NC-3.1	2	47	33.6	500	3.1	2.0	2.9	4.9
CII-SCC-6.3	2	49	33.9	1000	6.3	2.0	2.8	4.8
CII-NC-6.3	2	47	33.6	1000	6.3	2.0	2.8	4.8

f'_c : Compressive strength of concrete; E_c , E_s : Modulus of elasticity of concrete and steel, respectively; f_y , f_{yr} : Yield strength of steel tube and rebar, respectively



Note: all dimensions are in millimeters

Fig. 1 Details of Series II columns showing reinforcements

premature crushing of the concrete at the top and bottom of columns, longitudinal rebars were bent at 90° and directed outwards to the steel tube (Fig. 1). Bent longitudinal bars at the top and bottom

Table 2 Fresh and hardened properties of SCC and NC

Concrete type	Slump	Slump flow	Flow time	L-Box	Compressive strength (MPa)		
	mm	mm	sec	mm	2-day	7-day	28-day
SCC	-	655-695	3.2-3.9	0.70-0.77	32	42-44	49-54
NC	130-150	-	-	-	34	36-38	47-52

SCC: W/B: 0.41; cement = 453; water = 185; C. agg. = 729; Fine Agg. = 1060 (kg/m³); SP = 0.75%; VMA = 0.05%

NC: W/B: 0.41; cement = 486; water = 201; C. agg. = 1028 ; Fine Agg. = 647 (kg/m³); SP = 0%; VMA= 0%

of the column were tack welded to the steel tube just to keep the reinforcement cage in position but the welds were not strong enough to transfer axial load applied to the concrete core to the steel tube.

Proportions of SCC and NC mixtures are summarised in Table 2. All concrete mixtures were designed for a targeted 28-day compressive strength of approximately 50 MPa although SCC mixtures had lower coarse aggregate and higher fine aggregate quantities than NC. Type 10 Canadian Portland cement similar to ASTM Type I cement with specific gravity of 3.17 and Blain fineness of 4700 cm²/g was used. Local natural sand having a specific gravity (SSD) of 2.71, water absorption of 0.75%, and a fineness modulus of 2.6 was used as fine aggregate. 12-mm maximum size crushed gravels having a specific gravity of 2.64 and water absorption of 1.89% were used as coarse aggregate. A naphthalene formaldehyde sulphonic acid based superplasticizer (SP) with a solid content of 40.5% and a specific gravity of 1.21 was used in the SCC mixtures. A novel polysaccharide-based VMA in liquid form having specific gravity of 1.42 and total solid content of about 81% was used (Lachemi *et al.* 2003).

The fresh properties and compressive strengths (f'_c) of SCC and NC mixtures are summarized in Table 2. Flowability, deformability and flow characteristics (through restricted area) of SCC were determined by slump flow (Nagataki and Fujiwara 1995), V-funnel flow (Ozawa *et al.* 1994) and L-Box (Sonebi *et al.* 2000) tests respectively while traditional slump test was performed for NC. Slump flow, flow time and L-box index values (Table 2) satisfied recommended values needed for a SCC. The compressive strength of SCC and NC were determined from 100 mm × 200 mm control cylinders for each batch.

Both SCC and NC mixtures were mixed in a 100-L capacity batch mixer at Ryerson University concrete materials laboratory. Immediately after preparation, tests on fresh properties of the concrete mixtures as well as casting of CFST columns were carried out. SCC columns in Series CI and CII were cast without consolidation while NC columns were consolidated by external vibrators. The observed lower casting time and ease of consolidation in SCC columns will translate into the reduction of construction time and manpower on a full size construction project. Following casting, the specimens were cured in a humidity chamber for approximately 24 days and removed 3 days prior to testing at 28 days.

Strain gauges were installed on the steel surface at specific locations to monitor the development of axial and transverse strains throughout the loading history (Fig. 2).

CFST columns were tested in a 4600-kN MTS frame at the Ryerson University Structures Laboratory by applying axial compression forces only through the concrete core. Typical test set-up for CFST columns is shown in Fig. 2. Axial load, axial displacement and strains were recorded by a computer aided data acquisition system throughout the loading history until the failure of columns.

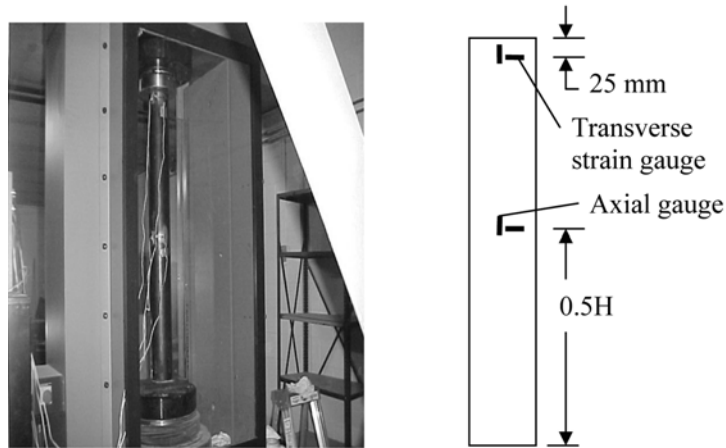


Fig. 2 Experimental set-up and instrumentation of columns

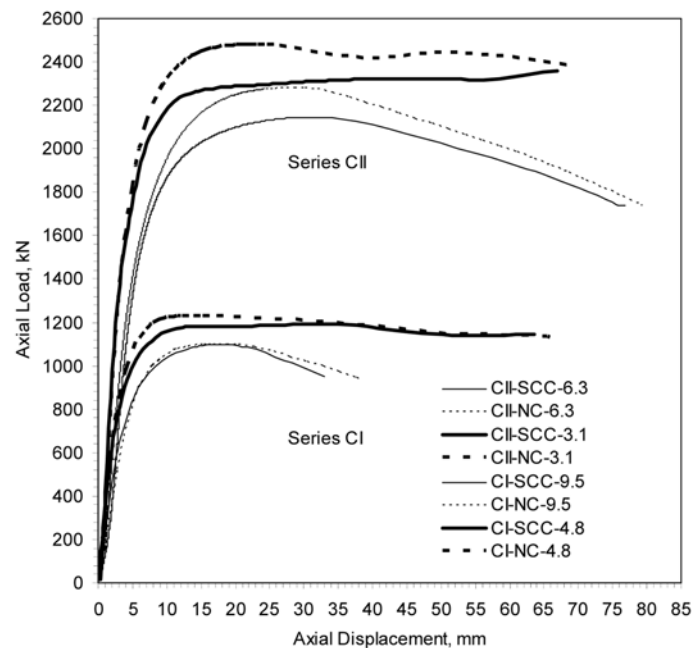


Fig. 3 Load-displacement responses of CFST columns

4. Load-displacement response and failure modes of CFST columns

Axial load - displacement responses of Series CI and CII columns are compared in Fig. 3. No significant difference in pre-peak, post-peak and ductility behavior was observed between NC and SCC columns. All columns showed outstanding ductility before failure. Two types of failure were observed based on the slenderness ratio (H/D). The steel tube was under lateral pressure due to its interaction with the axially loaded concrete core and was forced to undergo local buckling allowing lateral pressure to decrease at the section concerned. The presence of hoop and longitudinal steel

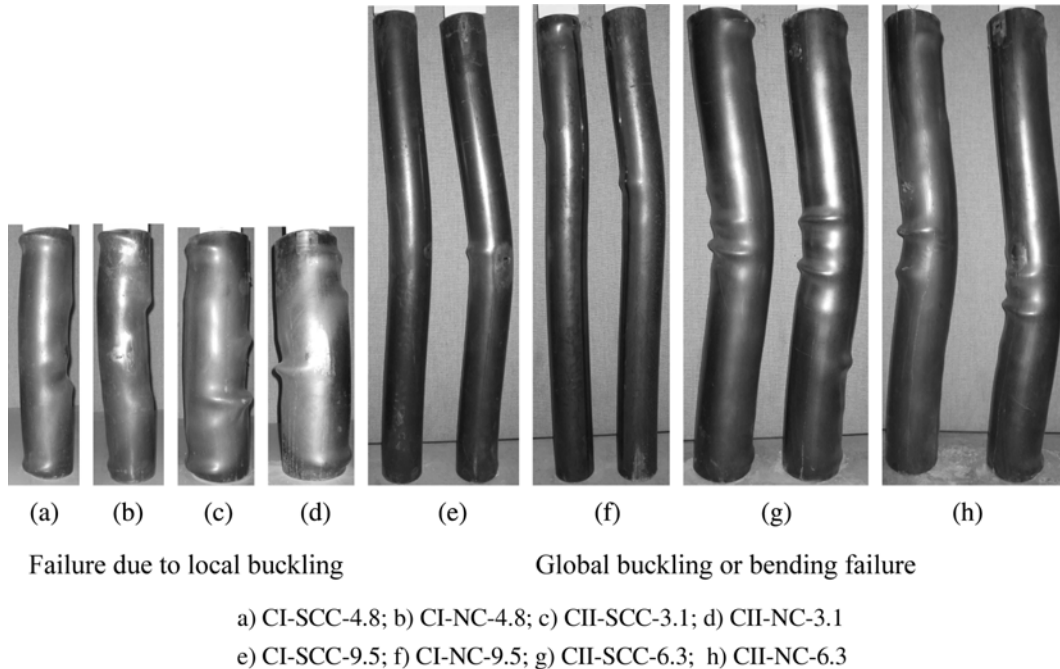


Fig. 4 Failure modes of CFST columns

provided better confinement and enhanced the strength and ductility of CII columns compared with CI columns. As loading continued, the initiation of first local buckling (short columns) or global buckling (slender columns) was noted. For short columns, the failure mode was the formation of successive local buckles with plastic yielding of steel and bending of columns as shown in Fig. 4(a)-(d). In short columns, local crushed concrete pushed the steel wall outward leading to an increase of lateral pressure in the steel that eventually led to the buckling and bulging out of the steel. A zone of plastic yielding (plastic hinge) was found in the steel tube between two adjacent buckles leading to bending and subsequent failure of the column (Fig. 4a-d). Comparatively, slender columns failed due to global buckling as shown in Fig. 4(e)-(h). However, for slender columns, initiation of global buckling associated with local buckles were started at the centre for SCC columns (Fig. 4e-f) while probably due to the non-homogeneity of concrete, the position of local buckle differed in NC columns (Fig. 4g-h).

In Series CI, NC columns generally showed higher strength over SCC columns by 4.1% and 1.1% for columns with H/D of 4.8 and 9.5, respectively (Fig. 3). In Series CII, NC columns generated higher strength over SCC columns by 7.5% and 6.3% for columns with H/D of 3.1 and 6.3, respectively (Fig. 3). The strength enhancement in NC columns (compared to SCC columns) was higher in CII columns compared with those in Series CI. However, the performance of SCC columns is found to be satisfactory in terms of strength compared with its NC counterpart as the maximum strength enhancement in NC columns ranged between 1.1% and 7.5% only.

Although the compressive strength of SCC (about 51 MPa) is slightly higher than NC (about 50 MPa), the reduction of strength in SCC columns compared with NC columns is thought to be due to the reduced shear friction or mechanical bond generated at the dilation of concrete in confined

circumstances in CFST columns. Since NC has higher quantity of coarse aggregate, its shear strength is higher compared with SCC due to higher shear friction along the shear path.

5. Biaxial stress development and confinement in CFST columns

5.1 Evolution of biaxial stress

Confined columns those are axially loaded through concrete core, expose the concrete to triaxial confinement (Hossain 2003, McAteer 2004). The steel tube is in a state of biaxial stress and the confining action of the steel tube begins after the concrete softens or dilates. The combination of stresses in the steel tube is shown in Fig. 5, where the transverse stress is a direct result of lateral pressure (f_2) acting on the steel tube from the confined concrete. The yield stresses of the steel tube as per von Mises failure criterion can be defined by Eq. (1):

$$f_{ys}^2 = \sigma_a^2 + \sigma_h^2 - \sigma_a \sigma_h \quad (1)$$

where σ_a , σ_h are the axial and transverse stresses in the steel tube, respectively; f_{ys} is the von Mises yield stress of the steel tube.

The biaxial stresses (σ_a and σ_h) can be calculated from the experimental axial and transverse strains. The biaxial stress path of the von Mises criterion for $f_{ys} = 300$ MPa is illustrated in Fig. 6. The stresses of CFST would fall in the fourth quadrant due to axial compression in the steel tube and the circumferential tension due to outward pressure by confined concrete. The axial and transverse yield stresses in the steel tube are lower than the uniaxial yield stress, and their development depends on the configuration of CFST, materials and steel-concrete interfacial bond.

The steel tube is considered yielded when $f_{ys} = f_y = 300$ MPa. Typical biaxial stress state at mid-height of SCC and NC columns based on the von Mises criterion is shown in Fig. 7. The comparative development of bi-axial stress (Fig. 7) shows more or less similar bi-axial stress condition in SCC and NC columns. At the initial stage of loading, only axial stresses are developed in the tube. At the yield of steel tube, transverse stresses are well developed but still axial stresses

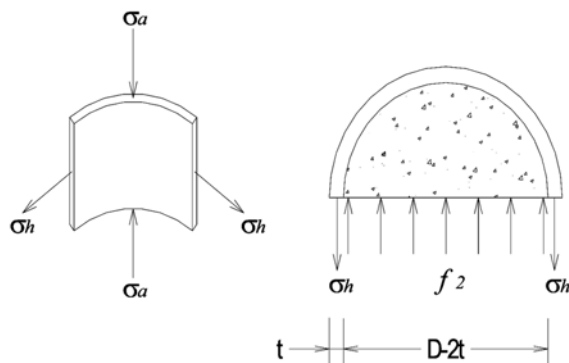


Fig. 5 State of stress in a confined column

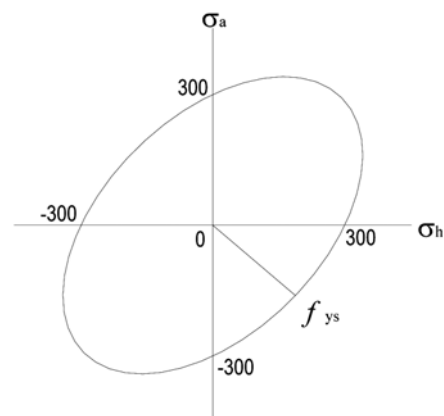


Fig. 6 von Mises stress path, $f_y = 300$ MPa

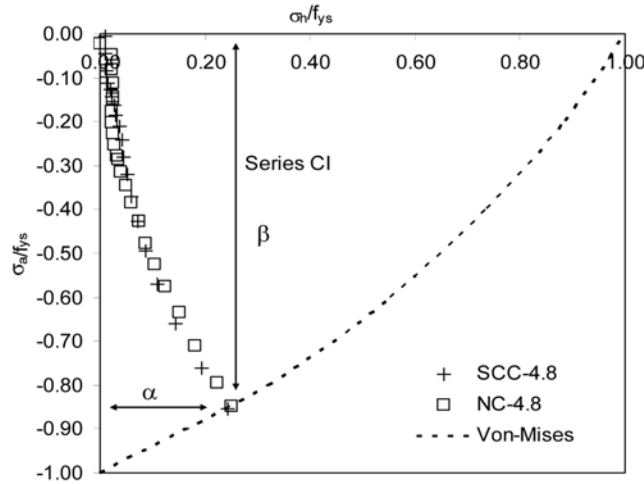


Fig. 7 Development of biaxial stresses in SCC and NC CFST columns

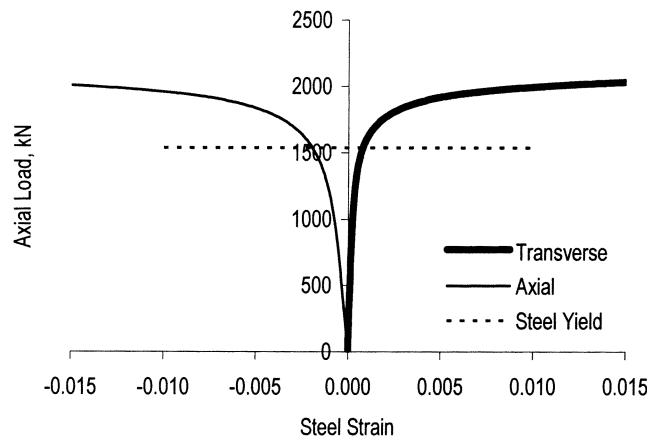


Fig. 8 Typical steel tube strain-column load evolution – CII-SCC-6.3

dominate. This suggests that axial load applied to the concrete is transferred to the steel tube. Following the steel yield, confining forces in the concrete began to increase the transverse strain in the steel tube at a rate equal to the axial strain. Typical evolution of steel tube strain in a SCC column is demonstrated in Fig. 8. NC columns also showed similar development.

The values of α and β , as illustrated in Fig. 7, are used to quantify axial (σ_a) and transverse (σ_h) stresses to the von Mises yield strength of steel (f_{ys}). α and β factors were calculated from charts similar to those shown in Fig. 7 for each column and used to analyze the stress relations for NC and SCC CFST columns. The predicted stress factors (α and β) for SCC and NC are listed in Table 3. The results are represented as a range based on type of column, type of concrete and H/D ratios.

The quantified axial and transverse stresses in the steel tube at bi-axial steel yield are then represented by Eqs. (2) and (3):

$$\sigma_a = \beta f_{ys} \tag{2}$$

Table 3 Stress factors for SCC and NC

Series	Concrete	H/D	Range (absolute values)	
			α	β
CI	SCC	4.8-9.5	0.23-0.21	0.87-0.88
	NC		0.24-0.15	0.86-0.92
CII	SCC	3.1-6.3	0.22-0.08	0.88-0.96
	NC		0.30-0.11	0.81-0.94

$$\sigma_h = \alpha f_{ys} \quad (3)$$

In Series CI columns, stress factors are very similar for both SCC and NC although NC columns tend to have less confining stresses as slenderness increases. This suggests that NC has less dilation over SCC. However, this effect is not repeated in CII columns, but somewhat reversed. In short columns of Series CII, NC shows greater confining stresses over SCC. The confinement stresses decrease at steel yield with the increase of slenderness in both SCC and NC columns. This can be attributed to the presence of additional hoop confinement. The increased confinement reduced the concrete dilation resulting in much higher peak loads than those observed in columns of Series CI.

When CFST column is loaded, the confinement effect does not begin until the concrete starts to dilate. The confinement pressure increases when the lateral expansion due to Poisson's effect and micro-cracking takes place. Therefore, confining stresses should reach peak values when the confined steel, has yielded. Lateral pressure developed by the dilation of concrete in the confined column can be obtained by Eq. (4) where the equilibrium in Fig. 5 is satisfied:

$$f_2 = \frac{2t}{D-2t} \sigma_h \quad (4)$$

where t and D are the thickness and outside diameter of the steel tube, respectively.

By substituting Eq. (3) in Eq. (4), the magnitude of lateral pressure of the confined concrete can be derived as:

$$f_2 = \frac{2t}{D-2t} \alpha f_{ys} \quad (5)$$

The hoop confined core of Series CII columns reduces the lateral pressure acting on the steel tube. Thus, to quantify the pressure exerted in the column as a whole, the hoop core pressure must be added. The lateral confining stress for the hoop confined concrete (f_{2h}) can be calculated as:

$$f_{2h} = \frac{2A_{sr}f_{yr}}{D_c s} \quad (6)$$

where A_{sr} and f_{yr} are section area and yield strength of the steel bar; D_c is the diameter of the concrete core and s is the lateral spacing of the confining hoops.

The maximum uniaxial lateral pressure ($f_{2\max}$) is calculated based on Eq. (7) at steel yield:

$$f_{2\max} = \frac{2t}{D-2t} \alpha f_{ys} + \frac{2A_{sr}f_{yr}}{D_c s} \quad (7)$$

Table 4 Observed steel yield and lateral stresses

Column	Average values for each pair of columns								
	P_{\max} kN	ε_p 10^{-6}	P_{ys} kN	ε_{ys} 10^{-6}	P_y/P_{\max}	$\varepsilon_{ys}/\varepsilon_p$	f_2 Eq. (5) MPa	f_{2h} Eq. (6) MPa	$f_{2\max}$ Eq. (7) MPa
CI-SCC-4.8	1173	23510	785	5768	0.67	0.25	5.8	-	5.8
CI-SCC-9.5	1091	13745	711	3945	0.65	0.29	5.3	-	5.3
CI-NC-4.8	1223	24510	788	5559	0.64	0.23	6.0	-	6.0
CI-NC-9.5	1103	13590	831	4900	0.74	0.35	3.8	-	3.8
CII-SCC-3.1	2283	30300	1510	7190	0.66	0.24	3.6	12.9	16.5
CII-SCC-6.3	2111	22700	1415	5052	0.67	0.22	1.3	11.9	13.2
CII-NC-3.1	2468	31530	1582	7690	0.64	0.24	4.8	12.9	17.7
CII-NC-6.3	2253	22120	1337	4930	0.59	0.22	1.8	11.9	13.7

Table 4 compares the axial peak load (P_{\max}) and peak strain (ε_p), axial load (P_{ys}) and strain (ε_{ys}) at biaxial steel yield, and the calculated lateral pressures (f_2 , f_{2h} , $f_{2\max}$) exerted by the confined concrete. The concrete lateral pressure (f_2) in columns CI is determined by Eq. (5). The higher lateral stress (f_2) for CII-NC-3.1 may be explained by the bond-slip aspect of the steel-concrete interface resulting in the lower axial stress transfer to the steel tube.

The maximum uniaxial lateral pressure for Series CII columns includes additional lateral pressure due to hoop confinement based on Eq. (7). The lateral pressures (f_2) of Series CII columns derived from the steel tube alone are small. Therefore, the inclusion of hoop induced lateral pressure (f_{2h}) in the concrete core (Eq. 6), reasonably describes the internal action of the confined columns of series CII (Table 4). Excluding the hoop effect would greatly underestimate the internal pressures acting on the concrete core for CII columns.

The values of P_{ys}/P_{\max} of CFST SCC columns were found similar (ranges between 0.65 and 0.67 for CI while between 0.66 and 0.67 for CII) and column configuration or slenderness seemed to have no effect. On the other hand, comparatively wider variations (between 0.64 and 0.74 for CI and 0.59 and 0.64 for CII) were observed in NC columns particularly with slender ones. This less variation of P_{ys}/P_{\max} can be attributed to the consistent performance of SCC (compared with NC) which is related to its better material characteristics such as homogeneity and self-consolidation. The inconsistent values of (P_{ys}/P_{\max}) for NC columns may lead to the erroneous strength prediction using analytical models. In this regard, SCC columns will be a better choice for the designers to avoid such discrepancies.

5.2 Quantification of concrete confinement

Although CFST columns were loaded through the concrete core, the biaxial stress actions in the steel tube indicates that a portion of the load is carried by the steel tube itself. The interfacial bond strength and tube configurations determine the magnitude of axial load transfer from the concrete to the steel tube. An increased bond strength effectively increases the stiffness of the CFST columns (McAtter *et al.* 2004). Due to the development of biaxial stresses, it is possible to determine the load carried by the steel and concrete through stress-strain measurement in the steel. The nominal

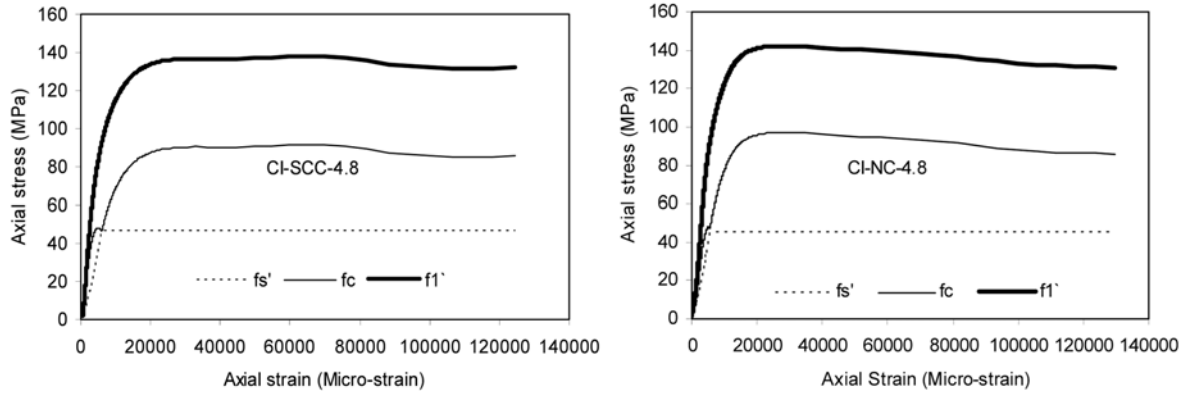


Fig. 9 Typical composite column response

axial stress (f_1') in the column when load (P) is applied to the concrete core can be taken as:

$$f_1' = \frac{P}{A_c} = \frac{P_c + P_s}{A_c} = f_c + \frac{\sigma_a A_s}{A_c} = f_c + f_s' \tag{8}$$

where P_s = load carried by the steel; P_c = load carried by concrete; f_c = stress in confined concrete; f_s' = equivalent axial stress transferred to steel tube, A_c = area of concrete core and A_s = cross-sectional area of steel tube. f_c and f_s' can be written as:

$$f_c = \frac{P}{A_c} - f_s' \tag{9}$$

$$f_s' = \frac{A_s \sigma_a}{A_c} \tag{10}$$

The stress-strain response of the confined concrete was determined by using axial load equations Eqs. (9) and (10). The axial stresses in the steel tube were converted to equivalent concrete stresses and subtracted from the stress-strain values of the confined columns. Typical stress-strain curves for steel tube, confined concrete and composite section are illustrated in Fig. 9.

Table 5 Quantified concrete confined strength

Column	H/D	f_c' MPa	f_{cc}' MPa	f_{cc}'/f_c'
CI-SCC-4.8	4.8	54	90	1.66
CI-SCC-9.5	9.5	54	80	1.47
CI-NC-4.8	4.8	52	96	1.85
CI-NC-9.5	9.5	52	81	1.56
CII-SCC-3.1	3.1	49	83	1.69
CII-SCC-6.3	6.3	49	72	1.47
CII-NC-3.1	3.1	47	101	2.14
CII-NC-6.3	6.3	47	80	1.69

Generally, these curves were used to observe the behavior of axial load sharing between steel and concrete in CFST columns. Columns of both series CI and CII displayed similar response including a dip at the steel yield point (Fig. 9). This is believed to be an artifact arising from the assumed abrupt yield of the steel tube (McAteer *et al.* 2004). As noted previously, the yielding of the steel tube happened much earlier than the peak load of the column. Therefore, it is valid to assume that the peak stress of the confined concrete corresponds to the peak load of the confined column. The yield stress (at which concrete dilates) of the concrete was then extracted from the stress-strain response curves at the peak load of the columns. These values were taken as the observed confined concrete strength, f'_{cc} , and are listed in Table 5 with their corresponding unconfined concrete strength (f'_c).

The confined strength (f'_{cc}) of SCC is found to be lower than that of NC. Confined strength also decreases with the increase of slenderness of the columns (Table 5). Observed f'_{cc} of SCC in columns with H/D ranging between 6.5 and 9.5 is on average 20% less than columns with H/D ranging between 3.1 and 4.8. On the other hand, observed f'_{cc} of NC in columns with H/D ranging between 6.5 and 9.5 is on average 30 to 40% less than columns with H/D ranging between 3.1 and 4.8. However, the increase in f'_{cc} is inconsistent in NC columns (f'_{cc}/f'_c ranges between 1.56 and 2.14) compared with SCC columns (f'_{cc}/f'_c ranges between 1.49 and 1.69).

In addition, Series CII columns generate some added complexity to the load sharing condition of axial forces. The loading of the steel tube is directly measured as discussed, but the concrete core load is shared between the concrete and reinforcing steel. Load sharing of the hoop confined concrete core and tube confined concrete was not directly measured in this program. However, the analytical model to derive confined concrete strength (f'_{cc}) in CII columns should include the combined effect of hoop and tube confinement.

6. Analytical models for confined concrete strength

The confined compressive strength of concrete was modeled by many researchers (Richart *et al.* 1928, Mander *et al.* 1988, O'Shea and Bridge 2000). Generally, the models are based on two types of confinement: (i) active confinement and (ii) passive confinement. Active confinement consists of constant lateral stress acting on the concrete as the axial load is applied. Passive confinement is achieved through the use of circular hoops, spirals, or tubing as a kinematic restraint.

One of the earliest investigations was conducted by Richart *et al.* (1928) on plain concrete cylinders with active confinement and a model for the confined compressive strength of concrete (f'_{cc}) was developed by the use of hydrostatic fluid pressure as the confining action and was based on normal strength concrete. The model developed by Mander *et al.* (1988) is popular but it should be noted that it was developed for predicting the uniaxial stress-strain curve of hoop and spiral confined concrete. The concrete loaded confined columns develop biaxial stresses and the steel tube does not reach its uniaxial yield stress. Therefore, Mander's model may over estimate the confined strength of concrete in CFST columns. O'Shea and Bridge (2000) model took into account the development of biaxial stresses in the steel confining tube and was a modification of Mander *et al.* (1988) model where new numerical constants were incorporated based on test results.

6.1 Proposed models for f'_{cc} with steel tube confinement

The proposed models were based on models developed by O'Shea and Bridge (2000), Richart

et al. (1928) and Mander *et al.* (1988). The proposed models are:

$$f'_{cc(R)} = f'_c + \frac{8.2t}{D-2t} \alpha f_{ys} \quad (11)$$

$$f'_{cc(M)} = f'_c \left(2.254 \sqrt{1 + 15.88 \frac{t \alpha f_{ys}}{f'_c (D-2t)}} - \frac{4t \alpha f_{ys}}{f'_c (D-2t)} - 1.254 \right) \quad (12)$$

$$f'_{cc(O)} = f'_c \left(2.172 \sqrt{1 + 14.92 \frac{t \alpha f_{ys}}{f'_c (D-2t)}} - \frac{4t \alpha f_{ys}}{f'_c (D-2t)} - 1.228 \right) \quad (13)$$

where subscripts (R), (M) and (O) in f'_{cc} represent that these models are developed based on Richart *et al.* (1928), Mander *et al.* (1988) and O'Shea and Bridge (2000), respectively.

The proposed models (Eqs. 11-13) can be used with the values of α generated from the test results of CFST columns with various types of concrete. For CFST columns in the current study, the values of α can be taken from Table 3.

6.2 Proposed model for f'_{cch} with hoop confinement

The existing models developed by Richart *et al.* (1928), Mander *et al.* (1988) and O'Shea and Bridge (2000) are based on the confining action of the steel tube only and do not take into account the effect of confining hoops in the concrete core as is the case for CII columns. To account for the effect of hoop confinement, authors proposed models based on existing models. Authors introduced lateral stress generated by hoop confinement (f_{2h}) in the existing models in place of f_2 (Eq. 5) where f_{2h} can be calculated based on Eq. (6). The proposed models for the confined concrete strength due to hoop confinement (f'_{cch}) are:

$$f'_{cch(R)} = 4.1 f_{2h} = 8.2 \frac{A_{sr} f_{yr}}{D_c s} \quad (14)$$

$$f'_{cch(M)} = f'_c \left(2.254 \sqrt{1 + 15.88 \frac{A_{sr} f_{yr}}{f'_c D_c s}} - 4 \frac{A_{sr} f_{yr}}{f'_c D_c s} - 0.254 \right) \quad (15)$$

$$f'_{cch(O)} = f'_c \left(2.172 \sqrt{1 + 14.92 \frac{A_{sr} f_{yr}}{f'_c D_c s}} - 4 \frac{A_{sr} f_{yr}}{f'_c D_c s} - 0.228 \right) \quad (16)$$

6.3 Proposed model for combined steel tube and hoop confinement

To evaluate the combined effect of steel tube and hoop confinement and to derive proposed models for combined confined strength of concrete (f'_{cct}), the equations representing f'_{cch} (based on Eqs. 14-16) and f'_{cc} (based on Eqs. 11-13) are combined as Eq. (17):

$$f'_{cct} = f'_{cc} \left(\frac{A_{cc}}{A_c} \right) + f'_{cch} \left(\frac{A_{cch}}{A_c} \right) \quad (17)$$

where A_c is the area confined by the steel tube, A_{cc} is the area of the concrete only and A_{cch} is the area confined by the hoop confinement.

The proposed models for f'_{cct} due to combined steel tube and hoop confinement based on Eq. (17) are:

$$f'_{cct(R)} = \frac{A_{cc}}{A_c} \left[f'_c + \frac{8.2t}{D-2t} \alpha f_{ys} \right] + 8.2 \frac{A_{sr} f_{yr} A_{cch}}{D_c s A_c} \tag{18}$$

$$f'_{cct(M)} = \frac{A_{cc} f'_c}{A_c} \left(2.254 \sqrt{1 + 15.88 \frac{t \alpha f_{ys}}{f'_c (D-2t)}} - \frac{4t \alpha f_{ys}}{f'_c (D-2t)} - 1.254 \right) + \frac{A_{cch} f'_c}{A_c} \left(2.254 \sqrt{1 + 15.88 \frac{A_{sr} f_{yr}}{f'_c D_c s}} - 4 \frac{A_{sr} f_{yr}}{f'_c D_c s} - 0.254 \right) \tag{19}$$

$$f'_{cct(O)} = \frac{A_{cc} f'_c}{A_c} \left(2.172 \sqrt{1 + 14.92 \frac{t \alpha f_{ys}}{f'_c (D-2t)}} - \frac{4t \alpha f_{ys}}{f'_c (D-2t)} - 1.228 \right) + \frac{A_{cch} f'_c}{A_c} \left(2.172 \sqrt{1 + 14.92 \frac{A_{sr} f_{yr}}{f'_c D_c s}} - 4 \frac{A_{sr} f_{yr}}{f'_c D_c s} - 0.228 \right) \tag{20}$$

6.4 Validation of confined concrete strength models

The summary of the confined concrete strength derived from proposed models and experiments for Series CI and CII columns are presented in Tables 6 and 7, respectively. Eqs. (18)-(20) (based

Table 6 Validation of models for confined concrete strength: Series CI columns

Column	Confined concrete strength (f'_{cc}), MPa				Ratio			% Error		
	Test	Theoretical models			Theoretical/Test					
		Richart Eq. (11)	Mander Eq. (12)	O'Shea Eq. (13)	Eq. (11)	Eq. (12)	Eq. (13)	Eq. (11)	Eq. (12)	Eq. (13)
CI-SCC-4.8	90	77	86	79	0.87	0.96	0.89	12.1	3.3	10.1
CI-SCC-9.5	80	75	84	77	0.95	1.05	0.97	4.2	4.3	2.3
CI-NC-4.8	96	77	86	79	0.80	0.89	0.82	19.0	10.3	17.2
CI-NC-9.5	81	67	74	68	0.83	0.91	0.85	14.0	7.0	12.5

Table 7 Validation of models for confined concrete strength: Series CII columns

Column	Confined concrete strength (f'_{cct}), MPa				Ratio			% Error		
	Test	Theoretical models			Theoretical/Test					
		Richart Eq. (18)	Mander Eq. (19)	O'Shea Eq. (20)	Eq. (18)	Eq. (19)	Eq. (20)	Eq. (18)	Eq. (19)	Eq. (20)
CII-SCC-3.1	83	81	87	78	0.98	1.05	0.95	1.9	3.8	4.5
CII-SCC-6.3	72	71	74	67	0.99	1.03	0.93	0.9	1.9	4.9
CII-NC-3.1	101	85	91	82	0.84	0.91	0.82	15.9	9.5	18.4
CII-NC-6.3	80	71	75	68	0.89	0.94	0.85	8.5	4.9	11.8

on Eq. 17) were used to generate all values for columns of series CI and CII. Series I columns do not contain added confining hoops and thus by elimination of the appropriate values in Eqs. (18)-(20), they revert back to the respective Eqs. (11)-(13), respectively.

The models predicted the confined concrete strength of Series CI and CII SCC columns with better accuracy than those of NC columns. The errors generated for NC columns of both series CI and CII are rather inconsistent (ranges between 4.9 and 18.4%) compared with SCC columns (ranges between 0.9 and 4.5%). The comparison also shows that model based on Mander *et al.* predicted confined strength of concrete better than other two models.

The predicted confined concrete strength (f'_{cct}) of CII columns are made up of two components: tube confined concrete strength (f'_{cc}), and hoop confined concrete strength (f'_{cch}). The proposition of adding the effect of hoop confinement in analytical models yields better prediction. Otherwise, the use of only f'_{cc} would underestimate the confined concrete strength and hence the peak strength prediction. Although Mander *et al.* (1988) model yields better prediction, Richart *et al.* (1928) and O'Shea and Bridge (2000) models were also included to develop analytical models for the prediction of the peak strength of CFST columns.

7. Development of strength models for CFST columns

The strength or peak load of CFST columns is derived from the axial capacities of the confined concrete and the steel tube. Existing models and Code based procedures for the strength of CFST columns are studied.

7.1 Code based design procedures for CFST columns

7.1.1 CAN/CSA S16.1-94 (CSA 1994)

The axial load is assumed to be carried by the concrete and steel tube independently when acting as a composite column. The factored resistance C_{rc} of the composite column can be taken as:

$$C_{rc} = \tau C_r + \tau' C_r' \quad (21)$$

where C_r = factored compressive resistance of the steel tube = $\phi_s A_s f_y (1 + \lambda_s^{2n})^{-1/n}$; ϕ_s = steel material resistance factor = 1.0 (no material safety factor assumed); $n = 1.34$; $\lambda_s = \frac{KH}{r_s} \sqrt{\frac{f_y}{\pi^2 E_s}}$; r_s = radius of gyration of the steel tube; $\tau = \frac{1}{\sqrt{1 + \rho + \rho^2}}$ if $H/D < 25$, or $\tau = \tau' = 1$; $\rho = 0.02(25 - L/D)$; $C_r' =$ factored compressive resistance of concrete $0.85 \phi_c f'_c A_c \lambda_c^{-2} [\sqrt{1 + 0.25 \lambda_c^{-4}} - 0.5 \lambda_c^{-2}]$; ϕ_c = concrete material resistance factor = 1.0 (no material safety factor assumed); $\lambda_c = \frac{KL}{r_c} \sqrt{\frac{f'_c}{\pi^2 E_c}}$; r_c = radius of gyration of the concrete area; $E_c = \left(1 + \frac{S}{T}\right) 2500 (\sqrt{f'_c})$; S is the short term load; T is the total load on column; $\tau' = 1 + \left(\frac{25 \rho^2 \tau}{D/t}\right) \left(\frac{f_y}{0.85 f'_c}\right)$.

7.1.2 AISC-LRFD 1994 (AISC 1994)

This is based on the principles adopted by ACI code and based on the design equations of steel columns. Both steel tube and concrete core are converted to equivalent members, and then reduced by a factor based on the slenderness of the column. The critical stress F_{cr} is computed from the slenderness parameter λ :

$$F_{cr} = (0.658^{\lambda^2})f_{my} \text{ for } \lambda \leq 1.5 \text{ and } F_{cr} = \left(\frac{0.877}{\lambda^2}\right)f_{my} \text{ for } \lambda > 1.5 \quad (22)$$

where $\lambda^2 = \left(\frac{kL}{r_m \pi}\right)^2 \left(\frac{f_{my}}{E_m}\right)$; r_m is the radius of gyration of the steel tube; compressive strength of the composite section, $f_{my} = f_y + 0.85 \frac{A_c f'_c}{A_s}$; elastic modulus of the composite section, $E_m = E_s + 0.4 E_c \frac{A_c}{A_s}$.

The critical load P_{cr} is then calculated as:

$$P_{cr} = A_s F_{cr} \quad (23)$$

7.1.3 Eurocode 4 (1992)

The plastic resistance of the crosssection of the composite column with concentric loading is given by the sum of all the components, steel tube, concrete and longitudinal reinforcements. The Code is recommended for composite sections with concrete not exceeding an unconfined strength of 50 MPa. The Code assumes full interaction of all the components and the ultimate load ($N_{pl,Rd}$) can be taken as:

$$N_{pl,Rd} = A_s f_y + A_c f'_c + A_{sz} f_{yr} \quad (24)$$

where A_s , A_c and A_{sz} are the cross-sectional area of the steel tube, concrete and reinforcement in the axial direction, respectively; f_y , f'_c and f_{yr} are the yield strength of the steel tube, concrete strength and yield strength of reinforcing steel, respectively.

7.2 An existing model

Hossain (2003) proposed a model for axial capacity of concrete filled steel tubular columns. The model developed were based on von Mises failure criterion and the values of α (to calculate f'_{cc}) and β are based on the biaxial yield of the confining steel tube and evaluated through experimental tests (as in Table 3). The proposed axial capacity of CFST columns (N_u) is:

$$N_u = \beta A_s f_y + A_c f'_{cc} \quad (25)$$

The confined concrete strength (f'_{cc}) was determined by using Eq. (26):

$$f'_{cc} = f_p + 4.1 \frac{2t}{D - 2t} \alpha f_y \quad (26)$$

where f_p is the unconfined compressive strength of concrete. To maintain wide application, the following equation was proposed (Sun and Sakino 1998) for f_p :

$$f_p = 1.61(d)^{-0.1}f'_c \quad (27)$$

where d is the diameter of the confined concrete section in mm.

7.3 Proposed model for the strength of CFST columns

Proposed models were developed based on the model (Eq. 25) proposed by Hossain (2003) so that they can be applicable to both steel tube (CI columns) as well as combined steel tube and hoop steel confined columns (CII columns). The axial strength (P_{r1}) models based on Eq. (25) can be written as:

$$P_{r1(R.or..M.or..O)} = \beta A_s f_{ys} + A_{cc} f'_{cc(R.or..M.or..O)} + A_{cch} f'_{cch(R.or..M.or..O)} + A_{ra} f_{yr} \quad (28)$$

where A_{ra} is the total area of longitudinal rebars, $f_{ys} = f_y$ and f_{yr} is the yield strength of the steel rebars. For CSFT columns without hoop or spiral confinement the values of $f'_{cch} = A_{ra} = A_{cch} = 0$. These models are applicable to both CI and CII columns as many parameters concerning the presence of longitudinal and hoop reinforcements will be eliminated for CI columns.

7.4 Identification of the most suitable model for strength prediction

Table 8 presents the comparison of strength or peak loads predicted by proposed models (Eq. 28). Stress factors (α and β) generated from this study (Table 3) are used. All models predicted the axial strength of columns with reasonable accuracy. All models can be used to predict the axial strength of CFST columns either CI or CII configurations with SCC or NC. However, for a comparative study with existing models and Code based procedures, a model is selected based on the lowest overall error and consistency of prediction. The selected proposed model is $P_{r1(M)}$ (Eq. 28) with the Mander *et al.* (1988) confinement theory.

Table 8 Comparative study of strength prediction by proposed models

Column	P_{test}	Theoretical strength, kN (Eq. 28)			Theoretical, $P_{r1} / \text{Test}, P_{test}$		
	kN	Richart $P_{r1(R)}$	Mander $P_{r1(M)}$	O'Shea $P_{r1(O)}$	Richart $P_{r1(R)}$	Mander $P_{r1(M)}$	O'Shea $P_{r1(M)}$
CI-SCC-4.8	1173	1064	1140	1081	0.91	0.97	0.92
CI-SCC-9.5	1091	1052	1125	1068	0.96	1.03	0.98
CI-NC-4.8	1223	1055	1131	1071	0.86	0.92	0.88
CI-NC-9.5	1103	997	1058	1010	0.90	0.96	0.92
CII-SCC-3.1	2283	2325	2433	2270	1.02	1.07	0.99
CII-SCC-6.3	2111	2190	2245	2112	1.04	1.06	1.00
CII-NC-3.1	2468	2353	2474	2300	0.95	1.00	0.93
CII-NC-6.3	2253	2178	2246	2110	0.97	1.00	0.94
		% Error	CI	SCC	6	3	5
				NC	12	6	10
			CII	SCC	3	6	0
				NC	4	0	7

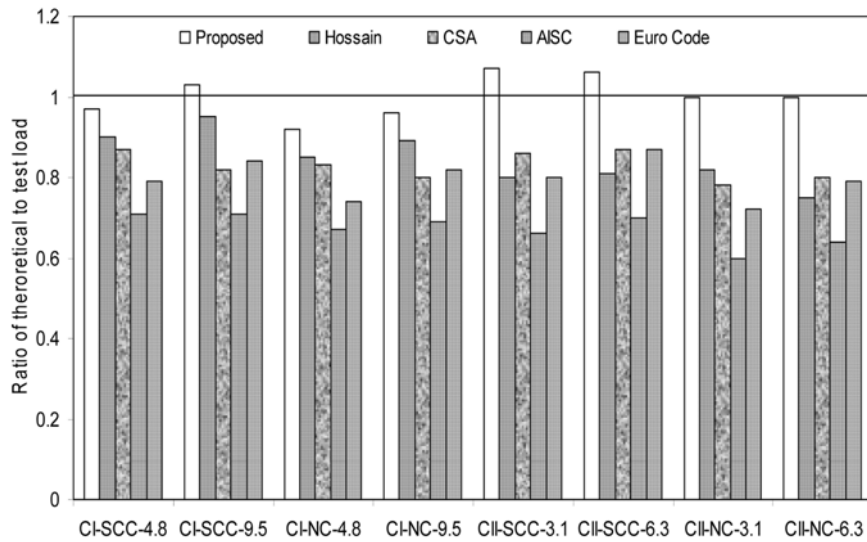


Fig. 10 Performance of the proposed model for prediction of strength

7.5 Performance of a proposed model in strength prediction

Fig. 10 compares the performance of theoretical models by showing the ratio of theoretical to test load (strength). It is found that the proposed selected model $P_{r1(M)}$ provides better prediction of axial strength for both CI and CII columns (ratio ranges between 0.96 and 1.03 for Series CI columns and between 1.0 and 1.07 for Series CII columns). The model proposed by Hossain (2003) was equipped with the stress factors (α and β) generated for the columns in this study (Table 3) while f'_{cc} was calculated based on Eq. (26). Notably, the model proposed by Hossain (2003) reasonably predicted the strength for Series CI columns (ratio ranges between 0.85 and 0.95) but under-predicted the strength of Series CII columns (ratio ranges between 0.75 and 0.81). Code based models of CSA (1994) (ratio ranges between 0.80 and 0.87 for Series CI and between 0.78 and 0.86 for Series CII), AISC (1994) (ratio ranges between 0.69 and 0.71 for Series CI and between 0.60 and 0.70 for Series CII) and Eurocode 4 (1992) (ratio ranges between 0.74 and 0.84 for Series CI and between 0.72 and 0.80 for Series CII) underestimated peak strengths of CFST columns. However, proposed selected model $P_{r1(M)}$ predicted the strength better than the model proposed by Hossain (2003).

The underestimation of strength especially for Series CII columns by the existing model proposed by Hossain (2003) and Code (AISC 1994, CSA 1994, Eurocode 1992) based equations was expected, because they do not take into account the effect of confining hoops or spirals. The proposed selected model appears to be good in predicting the axial strength of CFST columns with both SCC and NC. The comparative study validated the performance of the proposed selected model $P_{r1(M)}$ and hence the other proposed models too.

8. Conclusions

The axial load behaviour of concrete filled steel tube (CFST) columns cast with self-consolidating

concrete (SCC) and normal concrete (NC) were described. Columns were fabricated without and with longitudinal and hoop reinforcement (classified as Series CI and Series CII, respectively) in addition to the tube confinement. Evolution of biaxial stress in the steel tube and enhancement of concrete strength due to confinement were analysed to compare the performance of SCC and NC. Analytical models for the prediction of confined concrete strength and axial strength of CFST columns were developed and their performance was validated through test results, existing models and Code based design procedures. Based on the results presented in this paper, the following conclusions are drawn:

1. CFST columns made with SCC can develop comparable strength and ductility compared to those made with conventional NC. However, 1.1% to 7.5% strength enhancement in NC columns is attributed to the higher shear friction (a consequence of higher quantity of coarse aggregate in NC) generated at the dilation of concrete in a confined environment.
2. Biaxial stress development in the steel tube showed similar characteristics for both SCC and NC columns. Stress factors α and β are introduced to quantify axial (σ_a) and transverse (σ_h) stress based on the biaxial yield strength of steel tube (f_{ys}). For Series CI, the predicted stress factors are very similar for both SCC and NC although the development of less confining stresses with the increase of slenderness ratio (H/D) in NC columns suggests that NC has less dilation over SCC. In short CII columns, NC shows greater confining stresses and increased dilation over SCC. The confinement stresses decrease at steel yield for both SCC and NC when H/D increases which can be attributed to the presence of hoop confinement in such columns.
3. The ratio of biaxial yield (P_{ys}) and peak load (P_{max}) of CFST SCC columns ranges between 0.65 and 0.67 and column configuration and slenderness seemed to have no effect. On the other hand, comparatively wider variations ranging between 0.59 and 0.74 in NC columns can be attributed to the inconsistent performance of NC compared with SCC which can be related to SCC's better self-consolidation characteristics. This is an indication that greater homogeneity of distribution of in-place concrete properties along the height of the columns can be achieved by using SCC compared to NC.
4. The confined strength (f'_{cc}) of SCC is found to be lower than that of NC and f'_{cc} also decreases with the increase of slenderness of the columns. The value of f'_{cc}/f'_c in NC columns ranges between 1.56 and 2.14 compared with 1.49 and 1.69 of SCC columns.
5. Proposed analytical models are found good in predicting the confined concrete strength of both SCC and NC in CI and CII columns.
6. Performance of proposed models in predicting the axial strength of both CI and CII columns (with SCC or NC) is found to be better than existing models and Code based design procedures. Proposed models can be used with confidence in the design of SCC and NC CFST columns with or without added hoop or spiral reinforcement in practical situation.

References

- AISC (1994), "Manual of steel construction: Load and resistance factor design (LRFD)", 2nd Edition, American Institute of Steel Construction, Chicago, Illinois.
- Arima, I., Takeguchi, M., Sakurai, S. and Hayashi, J. (1994), "The quality of superworkable concrete used for the construction of Akashi-Kaikyo Bridge 4A Anchorage", *Proc. Japan Concrete Institute*, **16**(1), 25-30.
- Bouzoubaâ, N. and Lachemi, M. (2001), "Self-compacting concrete incorporating high volumes of class F fly

- ash: Preliminary results”, *Cement and Concrete Research*, **31**(3), 413-420.
- Campione, G., Mindess, S., Scibilia, N. and Zingone, G. (2000), “Strength of hollow circular steel sections filled with fibre-reinforced concrete”, *Canadian J. Civil Eng.*, **27**, 364-372.
- CSA (1994), “CAN/CSA S16.1-94: Limit states design of steel structures”, Canadian Standards Association, Rexdale, Ontario.
- Eurocode 4 (1992), “Design of composite steel and concrete structures, Part 1.1: General rules and rules for buildings”, ENV 1994-1-1.
- Gardner, N.J. and Jacobson, E.R. (1967), “Structural behaviour of concrete filled steel tubes”, *ACI J.*, **64**(7), 404-413.
- Hossain, K.M.A. (2003), “Behaviour of thin walled composite columns under axial loading”, *Composite – Part B: Engineering- An Int. J.*, **34**(8), 715-725.
- Hossain, K.M.A., Lambros, V.B. and Lachemi, M. (2004), “Concrete filled steel tubular columns cast with self-consolidating concrete-Experimental and theoretical investigations”, Research Report No. CRC-0401, Department of Civil Engineering, Ryerson University, Toronto, Canada, 54p.
- Khayat, K.H., Manai, K. and Trudel, A. (1997), “In situ mechanical properties of wall elements using self-consolidating concrete”, *ACI Mater. J.*, **94**(6), Nov-Dec, 491-500.
- Khayat, K.H., Paultre, P. and Tremblay, S. (2001), “Structural performance and in-place properties of self-consolidating concrete used for casting highly reinforced columns”, *ACI Mater. J.*, **98**(5), 371-378.
- Lachemi, M., Hossain, K.M.A., Lambros, V.B. and Bouzoubaâ, N. (2003), “Development of cost-effective self-compacting concrete incorporating fly ash, slag cement or viscosity modifying admixtures”, *ACI Mater. J.*, **100**(5), Sept.-Oct., 419-425.
- Lachemi, M., Hossain, K.M.A., Lambros, V.B., Nkinamubanzi, P.-C. and Bouzoubaâ, N. (2004a), “Performance of new viscosity modifying admixtures in enhancing the rheological properties of cement paste”, *Cement and Concrete Research*, **34**(2), 185-193.
- Lachemi, M., Hossain, K.M.A., Lambros, V.B., Nkinamubanzi, P.-C. and Bouzoubaâ, N. (2004b), “Self-compacting concrete incorporating new viscosity modifying admixtures”, *Cement and Concrete Research*, **24**(6), 917-926.
- Lahlou, K. and Aïtcin, P.-C. (1997), “Colonnes en beton a hautes performances confinee dans des enveloppes mince en acier”, Bulletin des Laboratoires de Ponts et Chaussées 209 (Mai-Jui) 49-67, (In French).
- Lahlou, K., Lachemi, M. and Aïtcin, P.-C. (1999), “Confined high strength concrete under dynamic compressive loading”, *J. Struct. Eng.*, ASCE, **125**(10), 1100-1108.
- Mander, J.B., Priestly, M.J.N. and Park, R. (1988), “Theoretical stress-strain model for confined concrete”, *J. Struct. Eng.*, ASCE, **114**(8), 1804-1826.
- McAteer, P., Bonacci, J.F. and Lachemi, M. (2004), “Composite response of high strength concrete confined by circular steel tube”, *ACI Struct. J.*, **101**(4), July – August, 466-474.
- Mei, H., Kiousis, P.D., Ehsani, M.R. and Saadatmanesh, H. (2001), “Confinement effects on high strength concrete”, *ACI Struct. J.*, **98**(4), 548-553.
- Nagataki, S. and Fujiwara, H. (1995), “Self-compacting property of highly flowable concrete”, ACI SP 154, Las Vegas, 301-314.
- O’Shea, M.D. and Bridge, R.Q. (2000), “Design of circular thin walled concrete filled steel tube”, *J. Struct. Eng.*, ASCE, **126**(11), 1295-1301.
- Ozawa, K., Maekawa, K., Kunishima, H. and Okamura, H. (1989), “Performance of concrete based on the durability design of concrete structures”, *Proc. of the Second East-Asia-Pacific Conference on Structural Engineering and Construction*, **1**, 445-456.
- Ozawa, K., Sakata, N. and Iwai, M. (1994), “Evaluation of self-compactibility of fresh concrete using funnel test”, *Proc. of JSCE*, No. 490, V-23, 1994.
- Patel, R., Hossain, K.M.A., Shehata, M. and Lachemi, M. (2004), “Development of statistical models for the mix design of high volume fly ash self-compacting concrete”, *ACI Mat. J.*, **101**(4), July-Aug., 294-302.
- Richart, F.E., Brandtzaeg, A. and Brown, R.L. (1928), “A study of the failure of concrete under combined compressive stresses”, Bulletin #185, University of Illinois, Engineering Experimental station, Urbana, Ill. 104 p.
- Shakir-Khalil, H. and Mouli, M. (1990), “Further tests on concrete-filled rectangular hollow section columns”,

- The Struct. Eng.*, **67**(19/3) Oct., 346-353.
- Sonebi, M., Batros, P., Zhu, W., Gibbs, J. and Tamimi, A. (2000), "Properties of hardened concrete", Task 4, Final Report (2000), Advance Concrete Masonry Center, University of Paisley, Scotland, UK. 6-73. (<http://scc.ce.luth.se>).
- Sun, Y.P. and Sakino, K. (1998), "Modeling for the axial behavior of high strength CFT columns", *Proc. 23rd Conf. on our World in Concrete and Structures*, 25-26 August, Singapore, 120-126.